Stark Effect Experiments in Cytochrome c-Type Proteins: Structural Hierarchies

M. Köhler,* J. Gafert,* J. Friedrich,* J. M. Vanderkooi,# and M. Laberge#
*Physikalisches Institut und Bayreuther Institut für Makromolekülforschung, Universität Bayreuth, 95440 Bayreuth, Germany, and #Johnson Research Foundation, Department of Biochemistry and Biophysics, School of Medicine, University of Pennsylvania, Philadelphia, PA 19104 USA

ABSTRACT We performed hole-burning Stark effect experiments on cytochrome *c* in which the iron of the heme was either removed or replaced by Zn. According to the experiments, the free-base compound has an effective inversion center, even in the protein. The Zn compound, on the other hand, shows quite peculiar features: in the low-frequency range of the inhomogeneous band, it definitely has a dipole moment, as indicated by a splitting of the hole in the external field. However, in the maximum of the inhomogeneous band, a severe charge redistribution occurs, as the experiments show. In addition to the Stark experiments, we performed calculations of the electrostatic fields at the pyrrole rings and at the metal site of the heme group. We interpret our findings with a model based on structural hierarchies: the protein can exist in a few subconformations, which can be distinguished through the structure of the heme pocket. The different pocket structures support different structures of the chromophore, which, in turn, can be distinguished through their behavior in an external field. These distinct structures, in turn, correspond to a rather broad distribution of protein structures, which leave, however, the pocket structure largely unchanged. These structures show up in inhomogeneous broadening.

INTRODUCTION

What is so fascinating about proteins is the fact that they reflect organization and randomness at the same time (Frauenfelder et al., 1988; Friedrich, 1995). It seems that both are needed for a sufficiently high level of complexity (Frauenfelder and Wolynes, 1994). Organization is, for instance, reflected in x-ray diffraction, whereas randomness is most directly reflected in inhomogeneous line broadening. It is a challenging problem in the optical spectroscopy of chromoproteins to unravel the nature of inhomogeneous line broadening. Inhomogeneous line broadening reflects all the conformational disorder in a protein. It has been suggested that, in proteins, disorder is organized in hierarchies (Ansari et al., 1985). It is an intriguing task to find out whether the various hierarchy levels correspond to different physical and/or functional properties as has been shown, for instance, for the so-called taxonomic states in myoglobin (Hong et al., 1990; Frauenfelder et al., 1991).

For the spectroscopist there are several problems. First, the different hierarchy levels may not be separated clearly enough in the spectrum. Second, it is not always straightforward to find a spectroscopically accessible parameter whose changes are sufficiently large to be clearly measured as one goes from one level to another.

Probably the most sensitive techniques of unraveling substructures in inhomogeneous line broadening and associated changes in physical properties are frequency-selective optical techniques, such as hole burning or photon echo techniques. With these techniques, inhomogeneous effects can be measured on the scale of the homogeneous linewidth (Friedrich and Haarer, 1984; Friedrich, 1990, 1991; Thorn Leeson and Wiersma, 1995; Thorn Leeson et al., 1994).

This paper presents a hole-burning Stark effect study on cytochrome *c*-type proteins. The Stark effect is very sensitive to the local field generated from the matrix at the probe site (Kohler et al., 1995; Gafert et al., 1995a,b). Given the protein structure, this field can be calculated by solving the Poisson-Boltzmann equation (Honig and Nicholls, 1995). The high sensitivity of the hole-burning Stark effect to the local matrix field gives rise to interesting aspects in protein spectroscopy; performing the experiment at several frequencies in the inhomogeneous band reveals whether the selected conformational substates are associated with changes in the local field at the chromophore site.

SPECIFIC ASPECTS OF A HOLE-BURNING STARK EFFECT EXPERIMENT

The Stark effect on spectral holes shows a quite specific feature—it is, as a rule, always linear in the external field, even if the probe molecule has inversion symmetry and does not possess a permanent dipole moment. The reason is that the field generated at the site of the probe by the matrix is orders of magnitude larger than the external field needed to change the shape and the center frequency of the hole (Maier, 1986; Meixner et al., 1986; Schätz and Maier, 1987; Kador et al., 1990). An order of magnitude measure of the ratio of internal and external field is the ratio of the inhomogeneous width to the hole width in an external field. Three cases are of interest:

1) The chromophore has inversion symmetry, the matrix is random. The Stark effect is determined through the dif-

Received for publication 18 December 1995 and in final form 19 March 1996.

Address reprint requests to Dr. Josef Friedrich, Physikalisches Institut, Universität Bayreuth, D-95440 Bayreuth, Germany. Tel.: 49-921-55-3245; Fax: 49-921-55-3250; E-mail: josef.friedrich@uni-bayreuth.de.

0006-3495/96/07/77/09 $2.00

ference of the induced dipole moments in the ground and excited states. This difference vector is random in magnitude as well as orientation. This randomness is not affected by the polarization of the hole-burning laser, and, consequently, a hole will broaden only in an external field, irrespective of the laser polarization.

2) The chromophore does not have inversion symmetry. As a rule, there will be a dipole moment difference vector with well-defined orientation. Polarized laser excitation creates a macroscopically anisotropic distribution of this difference vector, which can be controlled with respect to the external field by choosing the laser polarization in a proper way. If the main axis of this distribution is parallel to the Stark field, the hole will split. Hence, a splitting can be considered as the signature of a dipole moment difference vector with a well-defined orientation in the frame of the chromophore.

3) The chromophore has inversion symmetry, but the matrix is ordered. In this case, the matrix will induce a dipole moment with a well-defined orientation. This situation is equivalent to the presence of a permanent dipole moment. Hence, the hole will also split.

For proteins, the interesting conclusions come from a comparison with the behavior of the chromophore in a glass. From the glass spectra, it can be inferred whether the chromophore has inversion symmetry. If it has inversion symmetry, it can be broken by the protein in the sense that a macroscopic anisotropy of the dipole moment difference vector can be generated with polarized light excitation (Gafert et al., 1995a,b). If so, the field at the chromophore site must be dominated by the ordered structure of the protein and not by the randomness of the host glass. In this way, one gets information on the range of the relevant interaction of the chromophore with its environment. From a variation of the Stark pattern with burn frequency we learn that the structure of the protein must be different at the frequencies considered. In this way, one gets information on the correlation between frequency and structure and on the organization of the energy landscape.

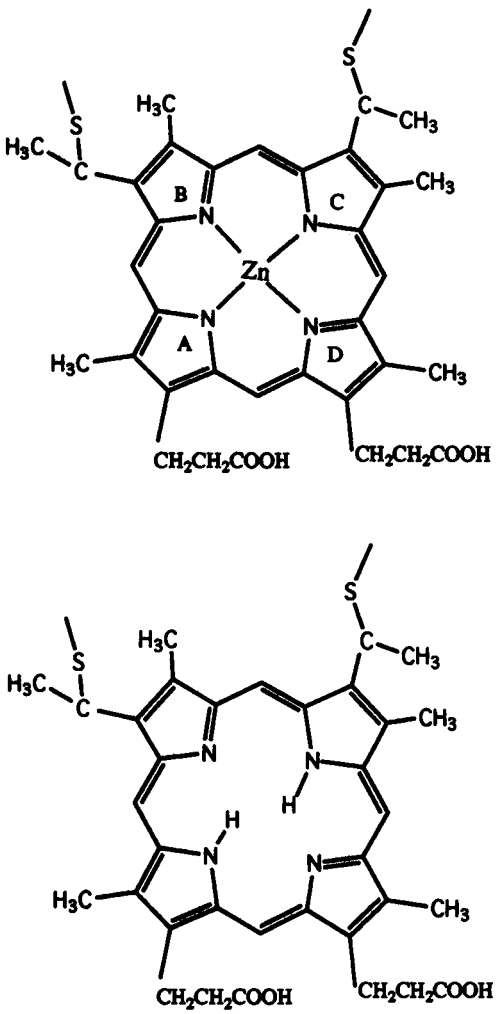

FIGURE 1 The chromophores. The letters designate the four porphyrin pyrrole rings. Note that the heme chromophores are covalently bound to the apoprotein through S linkages of cysteines.

MATERIALS AND METHODS

Spectroscopy and sample preparation

Zn and free-base cytochrome *c* were prepared as previously described (Vanderkooi et al., 1976). In cytochrome *c* the vinyl groups of protoporphyrin IX are condensed with cysteines to give a chromophore, as shown in Fig. 1 for the Zn and free-base derivatives.

The Stark effect experiments were performed for Zn-cytochrome *c* and the respective free base. For both chromophores we also performed the comparative experiments in a host glass. We chose dimethylformamide/glycerol in a volume ratio of 1:3. The protein was dissolved in a KH_2PO_4 buffer at pH 7. To ensure good optical quality of the sample, the buffer was mixed with glycerol in a volume ratio of 1:2. At the concentrations used, the ODs at the maximum of the long-wavelength band were 0.9 for Zn-cytochrome *c* (ZnCc) and 0.35 for free-base cytochrome *c* (H_2Cc). For Zn-protoprophyrin IX (ZnPP) and free-base protoporphyrin IX (H_2PP) dissolved in the glass matrix, the ODs were 0.9 and 0.12, respectively. The samples were sealed in glass cuvettes ($1 \times 6 \times 10$ mm^3) and placed between two electrodes. The respective voltage was varied between 0 and 7 kV, corresponding to a variation in the field between 0 and 11.7 kV/cm. The laser polarization was either parallel or perpendicular to the Stark field.

Hole burning was performed at 1.6 K with a single-frequency ring dye laser operated with rhodamine 6G. Holes were detected in transmission. Power levels and burning times were on the order of 100 μW and 100 s, respectively. To get sufficiently good signals, the holes were burned to relative depths of 30%. For the homogeneous linewidth experiments on ZnCc, we burned at each selected wavenumber a series of holes whose relative depths varied from 2 to 20%. The width of the hole extrapolated to zero area is twice the homogeneous linewidth.

The frequencies at which hole-burning Stark effect experiments were performed are marked with arrows (Fig. 2 and 5). For the zinc chromophore it suffices to show results at two different frequencies. For the free-base chromophore, no frequency dependence was found, either for the glass or for the protein, and thus we show results for one frequency only.

The usual data evaluation that we use in hole-burning Stark effect experiments, namely averaging over all the angular degrees of freedom as well as over some properly chosen distribution of induced dipole moments (Schätz and Maier, 1987), could not be applied to ZnCc because of the unusually sharp photoproduct peaks (Fig. 4). These experienced a shift in the Stark field as well, so that baseline problems occurred. Because of this, we will not compare absolute numbers but rather focus on the characteristic qualitative features.

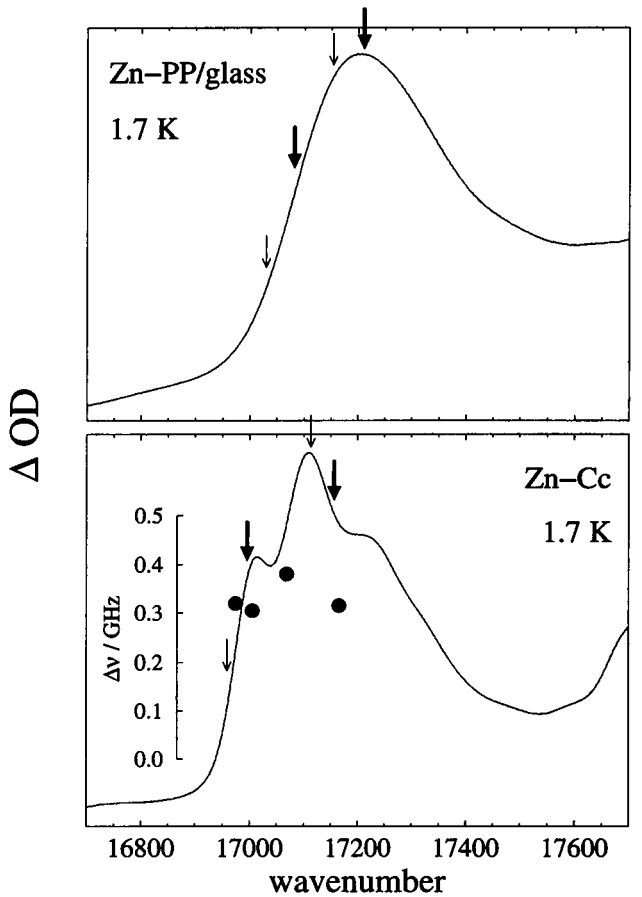

FIGURE 2 Inhomogeneously broadened long-wavelength absorption band of Zn-protoporphyrin (ZnPP) in a glass matrix and incorporated in cytochrome *c*. Arrows indicate frequencies where Stark effect experiments were performed. Fat arrows refer to the data shown in Figs. 3 and 4. The black dots show zero-fluence extrapolated hole width measurements.

COMPUTATIONAL METHODS

Energy minimization

Replacing the iron in cytochrome *c* with a zinc atom does not significantly affect the central metal environment (Anni et al., 1995, 1996), and we accordingly performed our calculations using coordinates generated from the x-ray structure of horse heart cytochrome *c*: pdb1hrc.ent (Bushnell et al., 1990), obtained from the Brookhaven Protein Data Bank (Bernstein et al., 1977). The energy was minimized using the Discover module of Insight II (Biosym Technologies, San Diego) on a Silicon Graphics IRIS Indigo workstation with the CVFF force field modified for the heme group (Laberge et al., manuscript submitted for publication). Missing hydrogens were added by using Discover (Biosym Technologies), subject to van der Waals constraints. In cytochrome *c*, only 7.5% of the total heme surface can directly interact with the solvent, and the heme group is deeply buried in the surrounding protein matrix, which eliminates the need to include the solvent explicitly in the minimization. However, because four of the protoporphyrin carbon atoms are exposed to the solvent (Bushnell et al., 1990), the x-ray waters were included. The minimization was performed by using a distance-dependent dielectric. The structure was first subjected to a steepest descent minimization to achieve a maximum derivative of less than 21 kJ mol^{-1}, followed by a conjugate gradient using a Newton-Raphson algorithm for which a residual maximum gradient of 0.42 kJ mol^{-1} was set as a convergence criterion.

Calculation of electric potential and field

The electrostatic potential and field of cytochrome *c* were calculated on the minimized structure at specific heme sites (Fe, NA, NB, NC, ND; see Fig. 1), using finite-difference Poisson-Boltzmann calculations as implemented in the Delphi software package (Gilson et al., 1988; Nicholls and Honig, 1991). This method has recently become a choice approach to solving the Poisson-Boltzmann equation for solvated molecules with complex charge distribution patterns, and we have recently used it to simulate the electrostatic field imposed by cytochrome *c* peroxidase on cytochrome *c* (Anni et al., 1995). The method has been fully described elsewhere (Gilson et al., 1988; Sharp and Honig, 1990). In classical electrostatics, the spatial variation in potential ϕ at position $\vec{r}$ is related to the charge distribution ρ and the position-dependent dielectric permittivity ϵ as follows:

$$\vec{\nabla}\epsilon(\vec{r})\vec{\nabla}\phi(\vec{r}) = -4\pi\rho/kT. \quad (1)$$

In the presence of ions, the Poisson equation can be combined with the Boltzmann equation, yielding:

$$\vec{\nabla}\epsilon(\vec{r})\vec{\nabla}\phi(\vec{r}) - \epsilon\kappa^2 \sinh(\phi(\vec{r})) = -4\pi\rho^f/kT. \quad (2)$$

The term κ^2 is equal to $1/\lambda^2$ or $8\pi q^2 I/ekT$, where λ is the Debye length, I is the ionic strength of the solution, q is the proton charge, and ρ^f is the fixed charge density. ϕ, ϵ, κ, and ρ are all functions of the vector $\vec{r}$, with the second term in the equation describing the salt effect. Two dielectric constants are used to take into account the solvation effect experienced by the charged groups of the protein in an aqueous solvent. In the algorithm used to solve Eq. 2, the solute-solvent variables were mapped on a three-dimensional grid (65^3) and charge, dielectric constant, and ionic strength (0.075 mM) were assigned to each lattice point. The longest dimension of the protein as a percentage of grid was 66%. Because ionic strength was taken into account, boundary conditions were set using the Debye-Hückel equation (Gilson et al., 1988). In the Delphi solution, the Poisson-Boltzmann equation is then replaced by a series of finite-difference equations, which are solved by iteration. The electrostatic energies are calculated as

$$\Delta G = \frac{1}{2}\sum_i q_i\phi_i, \quad (3)$$

where q_i is the charge and ϕ_i is the electrostatic potential at each atom i. The solute atomic charges and the van der

Waals radii are plugged into the calculation, along with the solute and solvent dielectric constants, 2 and 80, respectively (Young et al., 1993). The probe radius was set to 1.4 Å, and calculations were done on different scales and lattice mappings to ensure the uniformity of computational results. Graphics were produced using the GRASP software program (Nicholls et al., 1991).

Two calculations were performed. In the first, formal charges were assigned as follows: −0.5 to the Asp and Glu carboxyl oxygens, −0.5 to the oxygens of the two heme propionates, +0.5 to the Arg N_ζ and to both His N_δ and N_ϵ, and +1 to the Lys N_ζ. In the second calculation, the propionates were left uncharged.

RESULTS

Zn-cytochrome *c*

Fig. 2 compares the inhomogeneously broadened long-wavelength absorption band of ZnPP in a glass with ZnCc. Whereas the spectrum of the glass sample is smooth, the spectrum of the protein is structured. To elucidate the nature of this structure, we measured the quasi-homogeneous hole width for several frequencies across the two long-wavelength peaks of the inhomogenous band. It stays constant at 300 MHz. This value corresponds with a coherence time of >1 ns characteristic for a purely electronic origin. Hence, the first two peaks arise mainly from electronic origins, whereas the third and possibly higher peaks must correspond with vibrational transitions because we did not succeed in burning narrow holes into this part of the spectrum.

Fig. 3 shows holes burned at two different wavenumbers (bold arrows in Fig. 2) into the spectrum of the glass sample. Although the holes do not show a splitting, there is a clearly discernible tendency of a flattening of the shape of the hole for a polarization parallel to the Stark field as one goes from higher to lower frequencies. This flattening is indicative of a permanent dipole moment difference, although it is rather small.

Fig. 4 corresponds with Fig. 3. It shows the respective data of the protein. There is a striking feature: in the red edge of the band (16994 cm^{-1}) the hole clearly splits if the polarization of the laser is parallel to the Stark field. The high-frequency hole (17,155 cm^{-1}), however, just broadens, irrespective of polarization.

We want to point out a quite unusual feature: the spectrum shows sharply distributed photoproduct peaks with antihole character. At present it is not clear where these features come from. One possibility could be that they are due to rotational tunneling transitions in the methyl substituents, as they have been observed, for instance, in dimethyl-*s*-tetrazine in an *n*-alkane lattice (Orth et al., 1993). In any case, we know for sure that apart from such a narrow-bandwidth phototransformation, there is also a photoreversible broadband transformation that mutually converts the red and blue origins (Jira, 1995).

H_2-cytochrome *c*

Fig. 5 corresponds with Fig. 2. It compares the inhomogeneous absorption bands of H_2PP in a glass with H_2Cc. Again, the protein spectrum is structured, whereas the spectrum of the glass sample is smooth. Arrows indicate where hole burning was performed.

Figs. 6 and 7 show hole spectra in an electric field for the two samples. In both cases there is broadening only, irrespective of laser polarization, and there are no frequency-dependent features.

DISCUSSION

The inhomogeneous spectra

The inhomogeneous spectra show common features. For both chromophores the glass spectra are smooth, whereas

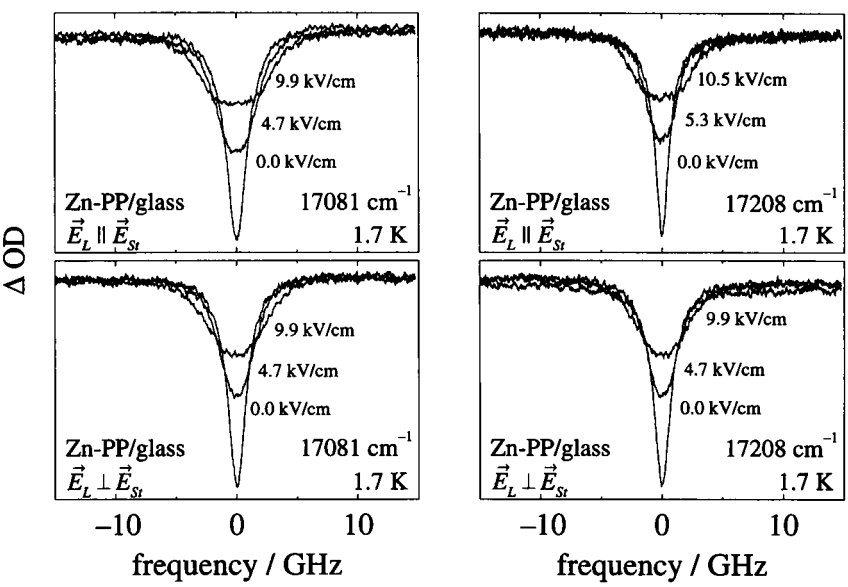

FIGURE 3 Stark effect on spectral holes of Zn-protoporphyrin IX in a glass matrix for two different frequencies. Polarization of the laser field is either parallel or perpendicular to the Stark field E_{st}.

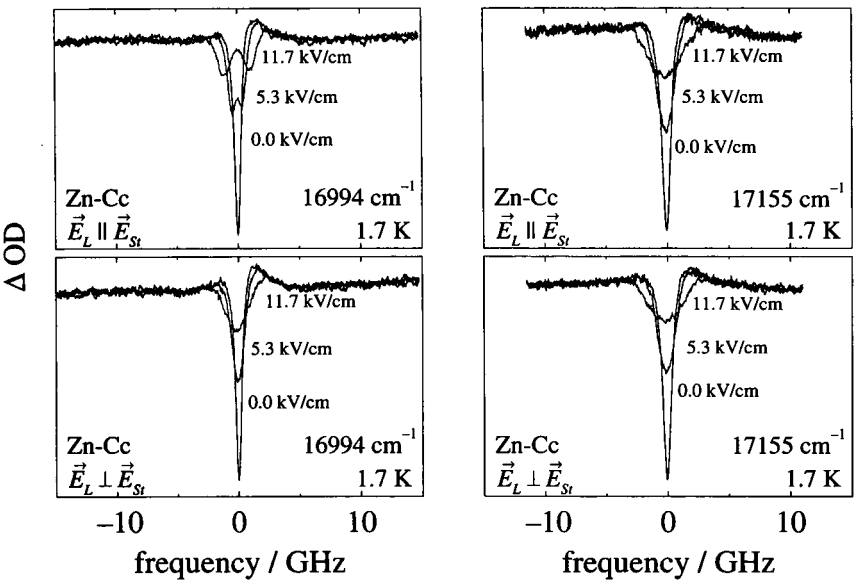

FIGURE 4 Stark effect on spectral holes of Zn-cytochrome *c* for two different frequencies. Polarization of the laser field is either parallel or perpendicular to the Stark field E_{st}.

the protein spectra are structured. As for the origin of this structure in H_2Cc, a straightforward argument would be that it corresponds with the inner ring tautomer states. However, the structure in the spectrum of ZnCc must be of a different nature. The homogeneous linewidth experiments support the presence of two electronic origins. They obviously correspond with two distinct structures of ZnCc. In this context it should be stressed that the "two origin" feature does not seem to be specific to ZnCc. We found two origins in all proteins substituted with Zn- and Mg-porphyrin derivatives that we have investigated so far. We suggest that the two structures are related to the two possible locations of the metal with respect to the molecular plane. The two positions can be distinguished through the asymmetry of the protein environment, which, in turn, induces an asymmetric charge distribution at the heme site. This can be demonstrated by calculating the electrostatic potential at the iron and at the

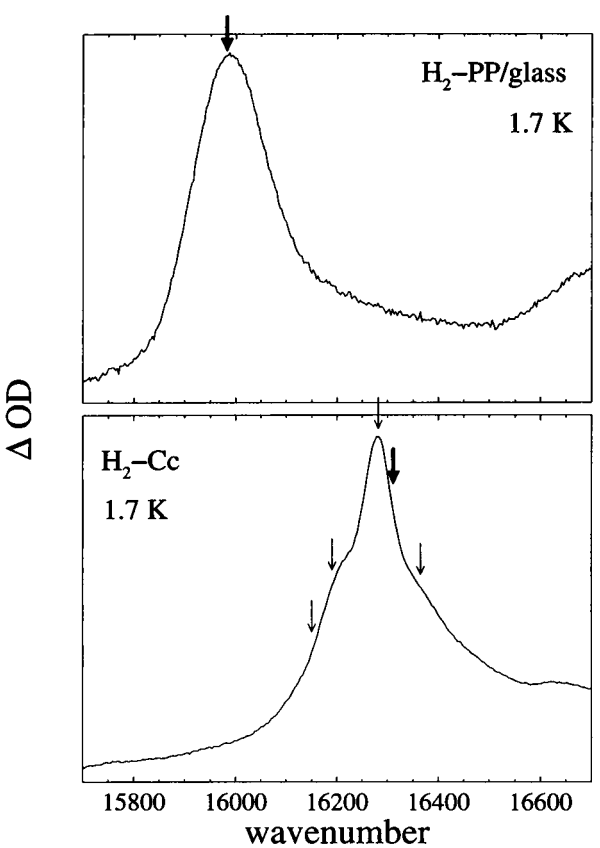

FIGURE 5 Inhomogeneously broadened long-wavelength absorption of free base protoporphyrin in a glass matrix and of free base cytochrome *c*. Arrows indicate frequencies at which Stark effect experiments were performed. Bold arrow refers to the data shown in Figs. 6 and 7.

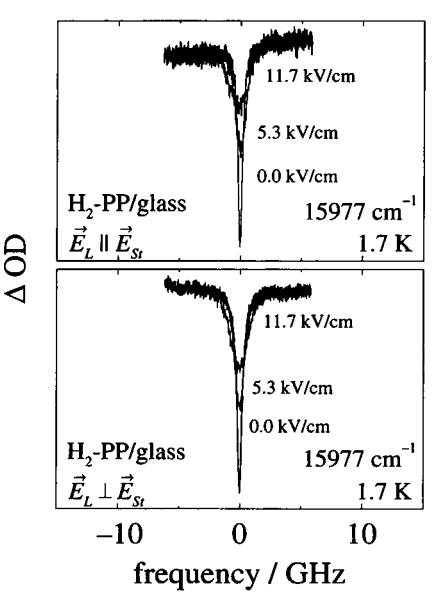

FIGURE 6 Stark effect on a spectral hole of free base protoporphyrin IX in a glass matrix. Polarization of the laser field is either parallel or perpendicular to the Stark field E_{st}.

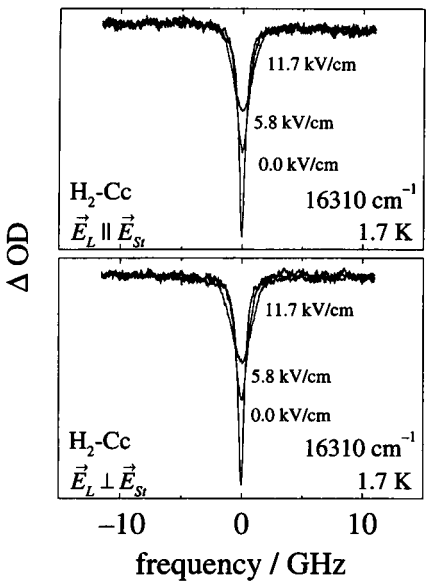

FIGURE 7 Stark effect on a spectral hole of free base cytochrome *c*. Polarization of the laser field is either parallel or perpendicular to the Stark field E_{st}.

four pyrrole nitrogens (NA, NB, NC, ND). The results presented in Table 1 and in Fig. 8 show that the electric field components and electrostatic potentials vary significantly for all sites considered, thus conferring a highly asymmetric charge distribution to the heme.

Switching the metal from one side of the heme plane to the other is likely to influence the nearby structure of the apoprotein. A mutual influence of apoprotein and prosthetic group structures seems to be a general phenomenon in protein physics. A well-studied example concerns the so-called taxonomic states in myoglobin (Frauenfelder et al., 1991).

TABLE 1 Effect of propionic acid charges on the electrostatic potential ϕ and electric field components E_i(i = x, y, z) calculated at specific heme sites (horse heart cytochrome *c*)

Site	ϕ (mV)	E_x(mV/Å)	E_y(mV/Å)	E_z(mV/Å)
Propionics charged				
Fe	−64	−22.3	−81.5	−60.0
NA	−225	−12.8	−148.8	−49.0
NB	27	−11.8	−37.3	−49.8
NC	43	−6.8	−29.0	−59.5
ND	−201	−51.5	−142.8	−58.5
Propionics uncharged				
Fe	335	11.0	22.5	−58.3
NA	360	−8.5	13.5	−39.5
NB	333	31.5	0.8	−65.5
NC	283	32.3	32.3	−55.3
ND	333	31.5	0.8	−65.5
Differences				
Fe	−399	−33.3	−104.0	−1.8
NA	−585	−4.3	−163.5	−9.5
NB	−56	−19.8	−37.8	−15.8
NC	−240	−25.5	−61.3	−4.3
ND	−534	−83.0	−143.5	−7.0

The heme is oriented to lie in the x,y plane with the central metal and the methine carbon bridging the B and C pyrrole rings (Fig. 1) lying along the y axis.

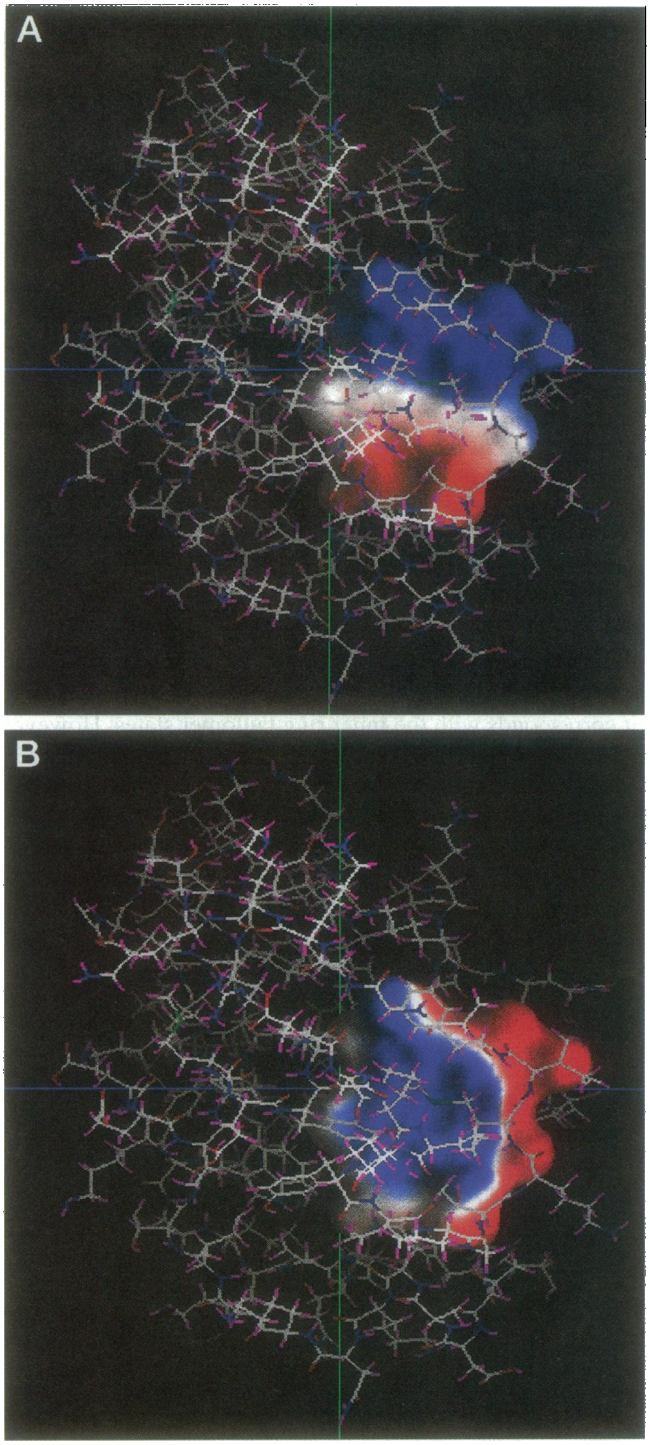

FIGURE 8 Electrostatic potential at the heme in horse heart cytochrome *c*. The molecular surface of the heme is color-coded according to its electrostatic potential: red is less than −125 mV and blue is more than −125 mV. All ionizable protein residues at pH 7 were charged according to their pK_a values. (*A*) Heme potential with propionic acids charged. (*B*) Heme potential with propionic acids uncharged.

Some aspects of the hole-burning phototransformation processes in metal porphyrins

For the free-base protoporphyrin we can safely assume that the hole-burning photoreaction is based on a light-induced rearrangement of the two inner-ring protons. This type of reaction has been verified for all free-base porphyrin molecules (Völker, 1987; Fidy et al., 1992). In low-temperature proteins there is quite a series of stable inner-ring protein configurations. However, in H_2Cc, only a few of them are populated at room temperature.

For the metal porphyrin we suggest the following mechanisms. In the presence of ligating donors, Zn-porphyrins are usually pentacoordinated and Zn is displaced out of the porphyrin plane toward the ligand (Schauer et al., 1985; Scheidt et al., 1986, 1987). For Zn-cytochrome *c*, NMR spectroscopy has shown that both ligands (i.e., Met and His) are in the same location as in the native ferrous cytochrome *c* (Anni et al., 1995). It is well known that, upon excitation, the ring widens, as has been experimentally verified by vibrational spectroscopy of Mg-porphyrin in myoglobin (Kaposi et al., 1993). We suppose, then, that the metal can penetrate the ring. Relaxation to the ground state restores the geometric barrier; hence the metal is again forced to dome. Either it goes back to its former position or it goes to the other side of the ring. In the first case nothing has changed. In the second case a photoproduct has been created that can be distinguished from the educt state, if the environment is asymmetric with respect to a reflection at the molecular plane. This view is in agreement with the above interpretation of the origin structure in the low-energy absorption band of ZnCc; there are two such states, corresponding with the metal being at one or the other side of the aromatic ring. The metal-switching photoreaction may also play a role in the glass matrix. But here, this reaction cannot be distinguished from photophysical hole burning.

Although we definitely know that the two origins can be mutually photoconverted, an additional hole-burning phototransformation process must be present, as is obvious from the sharp antihole-like photoproduct peaks that show up in the immediate neighborhood of the hole (Fig. 4). As suggested above, methyl group tunneling could be a possible explanation.

Stark effect experiments

The Stark effect experiments verify what we already surmised from the spectral features of the photochemistry: the protein molecules absorbing in the red edge of the inhomogeneous spectrum of ZnCc must be structurally different from those absorbing in the maximum. In the red edge, the chromophores definitely have a well-defined dipole moment, as documented by the splitting of the hole in an electric field. In the band maximum, the chromophores seem to have no net dipole moment.

How can this be understood? Let us first consider H_2PP in more detail (Figs. 6 and 7). It obviously does not have any significant dipole moment, either in the glassy solution or in the cytochrome *c* environment, because the hole does not split. Moreover, the field-induced broadening is quite small. From this we conclude that

1) the asymmetric substituents as well as the inner-ring protons do not perturb the π-electron system sufficiently strongly;

2) the polarizability of the free-base chromophore is obviously rather small;

3) in the protein, there seem to be no charged groups close enough to the chromophore to induce a sufficiently large dipole moment.

The conclusions are in line with the fact that H_2Cc does not show any frequency-dependent features in the Stark effect. Obviously, H_2PP is not a sufficiently sensitive Stark probe to feel any structural change in the Cc apoprotein. However, hole-burning pressure experiments reveal that there must be at least three different structures hidden beneath the inhomogeneous origins (Jira et al., to be published).

Upon comparing the Stark spectra of H_2PP and ZnPP in the glass matrix (Figs. 3, 6), we find that there are two obvious differences. First, the field-induced broadening in ZnPP is much stronger. As a consequence, the polarizability must be significantly higher. Second, there is a weak color effect. For the hole in the red edge (17,081 cm^{-1}) a clearly discernible flattening of the shape occurs at high field strength and with the laser polarized parallel to the Stark field. This flattening hints at a splitting of the hole, which, however, cannot be resolved because broadening is quite large. It is an indication of a permanent, albeit small, dipole moment. This dipole moment polarizes its solvent environment, which, in turn, creates a field at the probe site. This field enforces the original dipole moment. This interplay is stronger in the red edge of the inhomogeneous band because the solvent shift is stronger there. The consequence of this interplay is the weak color effect observed. It depends on the magnitude of the permanent dipole moment, the polarity of the solvent, and the polarizability of the chromophore.

We conclude that ZnPP has a permanent dipole moment, yet a small one. From its dependence on the laser polarization we conclude that this dipole moment has its major component in the molecular plane. Most probably the propionic acid groups lead to a displacement of the π-electron density. This view is in agreement with our field calculations at the central metal (iron) and at the four pyrrole nitrogens (NA, NB, NC, ND). The results are presented in Table 1 and Fig. 8 and they are quite conclusive. The charge on the propionic acid significantly affects both the electrostatic potential and the electric field components calculated at these sites. The fact that these field components do lead to an asymmetric charge distribution and, hence, to a dipole moment for ZnCc but not for the respective free-base protein is obviously due to the higher polarizability of the metal chromophore caused by the interaction of the electrons of

the metal with the π-electrons of the aromatic ring. We stress that this interpretation complies with triplet ESR experiments. These experiments show that the free base has a cylinder symmetry, whereas the ZnCc has not (Angiolillo and Vanderkooi, 1995).

In the Cc-protein the environment is less random as compared to the glass, the broadening induced by the local field is reduced, and the splitting due to the permanent dipole moment is easily resolved in the red edge band (Fig. 4).

However, going to the main peak (17155 cm^{-1}), the pocket structure must change because the Stark splitting vanishes and the respective broadening increases. The vanishing of the splitting indicates that the dipole moment difference vector experienced severe changes—either this vector decreased close to zero, indicating that the π-electron system of the chromophore is now characterized by an effective inversion symmetry, or the relative orientation between transition dipole moment and dipole moment difference vector changed in a way that a preferred orientation with respect to the Stark field can no longer be established. As our experiments show, the presence or absence of a splitting does not depend on frequency within the major peaks. We conclude that the severe changes of the dipole moment of the chromophore, by going from the red to the blue origin, result from switching the metal from the histidine to the methionine side of the ring or vice versa. Hence, the interaction of the metal atom with either the methionine or the histidine obviously changes the π-electron distribution in the aromatic ring in a way that the polarizing influence of the propionic acid groups is severely distorted.

CONCLUSIONS

Structures of proteins seem to be organized in hierarchies. This is shown by low-temperature spectroscopy of ZnCc. The inhomogeneous band reveals two peaks, separated by 96 cm^{-1}, which could be identified as electronic origins by measuring the associated homogeneous linewidths. Stark experiments revealed that these two origins differ in their pocket structure: in the low-energy origin the chromophore has a dipole moment, as is obvious from a clearly detectable splitting; in the high-energy origin, Stark spectroscopy did not reveal a splitting. Hence significant charge displacements must occur as the protein converts from one origin to the other. We suggested that these two origins correspond with the metal being located either on the methionine or on the histidine side. Because we found that the long-wavelength origin can be photoconverted into the short-wavelength one, light-induced metal switching is suggested as a possible photoreaction mechanism.

Apart from the two pocket states, there is a broad distribution of conformational substates of the apoprotein, as is obvious from inhomogeneous line broadening of the two origins. However, the conformational substates preserve the distinct pocket structures. This is deduced from the observation that the Stark spectra did not depend on frequency within the inhomogeneous band of either one of the two origins.

That similar things are not seen in the respective free-base compound does not mean that they are not there. On the contrary, the inhomogeneous spectra show a discrete band structure, but the associated conformational substates did not modify the charge distribution of the free-base chromophore, so that they could be characterized in more detail by Stark spectroscopy.

Support from the DFG (Graduiertenkolleg "Nichtlineare Dynamik und Spektroskopie"), from the "Fonds der Chemie," and from the National Institutes of Health (POI GM48130) is greatfully acknowledged.

REFERENCES

Angiolillo, P. J., and J. M. Vanderkooi. 1995. Electron paramagnetic resonance of the excited triplet state of metal free and metal substituted cytochrome *c*. *Biophys. J.* 68:2505–2518.

Anni, H. J., J. M. Vanderkooi, and M. R. Chance. 1996. Extended x-ray absorption fine structure studies of the zinc derivative of cytochrome *c*. *Biophys. J.* 70:A153.

Anni, H. J., J. M. Vanderkooi, and L. Mayne. 1995. Structure of zinc-substituted cytochrome *c*: nuclear magnetic resonance and optical spectroscopic studies. *Biochemistry.* 34:5744–5753.

Ansari, A., J. Berendzen, S. F. Bowne, H. Frauenfelder, I. E. T. Iben, T. B. Sauke, E. Shyamsunder, and R. D. Young. 1985. Protein states and proteinquakes. *Proc. Natl. Acad. Sci. USA.* 82:5000–5004.

Bernstein, F. C., T. F. Koetzle, G. J. B. Williams, E. F. Meyer, M. D. Brice, J. R. Rodgers, O. Kennard, T. Shimanouchi, and M. Tasumi. 1977. The protein data bank: a computer-based archival file for macromolecular structures. *J. Mol. Biol.* 1112:535–549.

Bushnell, G. W., G. V. Louie, and G. D. Brayer. 1990. High-resolution three-dimensional structure of horse heart cytochrome *c*. *J. Mol. Biol.* 214:585–595.

Fidy, J., J. M. Vanderkooi, J. Zollfrank, and J. Friedrich. 1992. More than two pyrrole tautomers of mesoporphyrin stabilized by a protein. *Biophys. J.* 61:381–391.

Frauenfelder H., F. Parak, and R. D. Young. 1988. Conformational substates in proteins. *Annu. Rev. Biophys. Biophys. Chem.* 17:451–479.

Frauenfelder, H., S. G. Sligar, and P. Wolynes. 1991. The energy landscapes and motions in proteins. *Science.* 254:1598–1603.

Frauenfelder, H., and P. Wolynes. 1994. Biomolecules: where the physics of complexity and simplicity meet. *Phys. Today.* 47:58–64.

Friedrich, J. 1990. Hole burning in biopolymers. *Mol. Cryst. Liq. Cryst.* 183:91–103.

Friedrich, J. 1991. Hole burning spectroscopy of chromoproteins. *In* Light in Biology and Medicine. R. H. Douglas, J. Moan, and G. Rontó, editors. Plenum Press, New York. 345–356.

Friedrich, J. 1995. Hole burning spectroscopy and physics of proteins. *Methods Enzymol.* 246:226–259.

Friedrich, J., and D. Haarer. 1984. Photochemical hole burning: a spectroscopic study of relaxation processes in polymers and glasses. *Angew. Chem. Int. Ed. Engl.* 23:113–140.

Gafert, J., J. Friedrich, and F. Parak. 1995a. Stark effect experiments on photochemical holes in chromoproteins. *Proc. Natl. Acad. Sci. USA.* 92:2116–2120.

Gafert, J., J. Friedrich, J. M. Vanderkooi, and J. Fidy. 1995b. Structural changes and internal fields in proteins: a hole burning study of horseradish peroxidase. *J. Phys. Chem. Lett.* 99:5223–5227.

Gilson, M., K. Sharp, and B. Honig. 1988. Calculating the electrostatic potential of molecules in solution: method and error assessment. *J. Comp. Chem.* 9:327–335.

Hong, M. K., D. Braunstein, B. R. Cowen, H. Frauenfelder, I. E. T. Iben, J. R. Mourant, P. Ormos, R. Scholl, A. Schulte, P. J. Steinbach, A.-H.

Xie, and R. D. Young. 1990. Conformational substates and motions in myoglobin. External influences on structure and dynamics. *Biophys. J.* 58:429–436.

Honig, B., and A. Nicholls. 1995. Classical electrostatics in biology and chemistry. *Science.* 268:1144–1149.

Jira, Th. 1996. Diploma thesis. University of Bayreuth.

Kador, L., S. Jahn, D. Haarer, and R. Silbey. 1990. Contribution of the electrostatic and the dispersion interaction to the solvent shift in a dye polymer system, as investigated by hole burning spectroscopy. *Phys. Rev.* B41:12215–12226.

Kaposi, A. D., J. Fidy, S. S. Stavrov, and J. M. Vanderkooi. 1993. Optical fine-structure investigation of chromophore/protein interactions: Mg protoporphyrin myoglobin. *J. Phys. Chem.* 97:6317–6327.

Kohler, B. E., R. I. Personov, and J. C. Woehl. 1995. *In* Laser Techniques in Chemistry. T. Rizzo and A. Myers, editors. Wiley, New York.

Maier, M. 1986. Persistent spectral holes in external fields. *Appl. Phys.* B41:73–90.

Meixner, A. J., A. Renn, S. E. Bucher, and U. P. Wild. 1986. Spectral hole burning in glasses and polymer films: the Stark effect. *J. Phys. Chem.* 90:6777–6785.

Nicholls, A., and B. Honig. 1991. A rapid finite difference algorithm utilizing successive overrelaxation to solve the Poisson-Boltzman equation. *J. Comp. Chem.* 12:435–445.

Nicholls, A., K. A. Sharp, and B. Honig. 1991. Protein folding and association: insights from the interfacial and thermodynamic properties of hydrocarbons. *Proteins.* 11:281–296.

Ormos, P., A. Ansari, D. Braunstein, B. R. Cowen, H. Frauenfelder, M. K. Hong, I. E. T. Iben, T. B. Sauke, P. J. Steinbach, and R. D. Young. 1990. Inhomogeneous broadening in spectral bands of carbonmonoxymyoglobin. *Biophys. J.* 57:191–199.

Orth, K., P. Schellenberg, and J. Friedrich. 1993. Spin conversion relaxation in dimethyl-*s*-tetrazine doped *n*-octane: deuteration and symmetry breaking. *J. Chem. Phys.* 99:1–6.

Schätz, P., and M. Maier. 1987. Calculation of electric field effects on persistent spectral holes in amorphous host-guest systems. *J. Chem. Phys.* 87:809–820.

Schauer, C. K., O. P. Anderson, S. S. Eaton, and G. R. Eaton. 1985. Crystal and molecular structure of a six-coordinate zinc porphyrin: bis(tetrahydrofuran)-(5,10,15,20-tetraphenylporphinato)zinc(II). *Inorg. Chem.* 24:4082–4086.

Scheidt, W. R., C. W. Eigenbrot, M. Ogiso, and K. Hatano. 1987. Stereochemistry of a porphyrin atropisomer. The molecular and crystal structure of six-coordinate [5a,10b-bis(*o*-nicotinamidophenyl)-15,20-diphenylporphinato]-zinc(II). *Bull. Chem. Soc. Jpn.* 60:3259–3533.

Scheidt, W. R., J. U. Mondal, C. W. Eigenbrot, A. Adler, L. J. Radonovich, and J. L. Hoard. 1986. Crystal and molecular structure of the silver(II) and zinc(II) derivatives of mesotetraphenylporphyrin. An exploration of crystal-packing effects on bond distance. *Inorg. Chem.* 25:795–799.

Sharp, K., and B. Honig. 1990. Electrostatic interactions in macromolecules: theory and applications. *Annu. Rev. Biophys.* 19: 301–332.

Thorn Leeson, D., O. Berg, and D. A. Wiersma. 1994. Low temperature protein dynamics studied by long-lived stimulated photon echo. *J. Phys. Chem.* 98:3913–3916.

Thorn Leeson, D., and D. A. Wiersma. 1995. Real time observation of low temperature protein motions. *Phys. Rev. Lett.* 74:2138–2141.

Vanderkooi, J. M., F. Adar, and M. Erecinska. 1976. Metallocytochrome *c*: characterization of electronic and emission spectra of Sn and Zn cytochromes *c*. *Eur. J. Biochem.* 64:381–387.

Völker, S. 1987. High resolution spectroscopy of organic solids: hole burning in molecular crystals and amorphous systems at low temperature. *In* Excited State Spectroscopy of Solids, XCVI Corso. Societa Italiana di Fisica. 363–417.

Yang, A.-S., M. R. Gunner, R. Sampogna, K.. Sharp, and B. Honig. 1993. On the calculation of pKa's in proteins. *Proteins.* 15:252–265.